International Journal of Computer Information Systems and Industrial Management Applications
ISSN 2150-7988 Volume 18(2) 2026 pp. 1426-1443
https://doi.org/10.70917/ijcisim-2026-4250
Article

M-LSA-Net: A Hybrid Morphology-Aware Deep Learning Framework for Lumpy Skin Disease Detection

Yashaswini K[1], Gowrishankar S[2]

[1]Department of Computer Science and Engineering, Dr Ambedkar Institute of Technology ,Affiliated to Visvesvaraya technological University, Bengaluru, India
Email: yashaswinikphd@gmail.com
[2]Department of Computer Science and Engineering, Dr Ambedkar Institute of Technology, Affiliated to Visvesvaraya Technological University, Bengaluru, India
Email: gowrishankarnath@acm.org

Abstract: Lumpy Skin Disease (LSD) is a highly contagious viral disease that significantly impacts livestock productivity and agricultural economies worldwide. Traditional diagnostic approaches, including manual inspection and laboratory testing, are often time-consuming, resource-intensive, and unsuitable for rapid field-level deployment. To address these limitations, this study proposes M-LSA-Net, a hybrid morphology-aware deep learning framework for accurate and efficient detection of LSD from cattle skin images. The proposed model integrates MixUp-based data augmentation for improved generalization, LUMPNet-based region-focused feature extraction for capturing lesion-specific patterns, an Attention-Based Sparse Autoencoder (AB-SAE) for adaptive feature selection, and a Morphology-Aware Deep Classifier (MADC) for capturing both local texture and global structural patterns. The model was evaluated on a publicly available dataset using an 80:20 train–test split and assessed using standard performance metrics. Experimental results demonstrate that M-LSA-Net achieves an accuracy of 98.71%, precision of 98.68%, recall of 98.71%, F1-score of 98.69%, and ROC-AUC of 0.9978, outperforming baseline models such as CoAtNet, SwinT V2, and MaxViT. The findings highlight the effectiveness of combining attention-based feature refinement and morphology-aware learning for robust disease detection, making the proposed framework suitable for real-world veterinary diagnostic applications.

Keywords: Lumpy Skin Disease, Deep Learning, Morphology-Aware Classification, Attention-Based Feature Selection, Image Classification, Veterinary Diagnosis

1. Introduction

Bovine species, such as water buffaloes and cattle, are susceptible to the lethal virus known as Lumpy Skin Disease (LSD), which may travel internationally. When it was first found in 1929 in Zambia, Southern Africa, medical professionals mistakenly thought it was a plant poisoning or insect stinging [1]. Although the illness did not reach Botswana until 1943, 8 million cattle were infected as it travelled over north-west Africa. In 1989, the illness reached Israel [2] thereafter, it extended to a number of Middle Eastern nations. Jordan Iraq and Turkey experienced disease outbreaks during 2013 which led to the first outbreak in Russia that occurred in 2015 [3]. The first Indian report of an epidemic occurred in Odisha in August of 2019; a second, more serious outbreak occurred in 2022, confirming the disease's Asian expansion [4].

Because it is a member of the Poxviridae family and the Capripoxvirus genus, the Lumpy Skin Disease Virus (LSDV) causes LSD. Although LSD directly poses no harm to human health, it is the most dangerous concern of the disease spreading among domestic and wild animals in perspective to farmers and veterinarians. Insects that feed on blood, such as ticks and mosquitoes, or coming into touch with infected animals or items are the main vectors for the virus's transmission [5]. Massive skin nodules, up to 5 cm in diameter, are the outward sign of the condition [6] and it

brings about symptoms which include fever and decreased milk production and reduced appetite and lameness and leg edema [7], [8]. Laboratory approaches for LSDV detection include viral isolation techniques and polymerase chain reaction (PCR) testing [9]. Presently, there is no antiviral therapy for LSD in medicine; instead, sick cattle must undergo supportive treatment with antibiotics, analgesics, and wound care sprays. There are a number of vaccinations that may be used to stop the spread of goat pox, including the Neethling vaccine, the KSGP O-180 strain vaccine, and the GTP vaccine. Traditional disease detection methods depend on veterinarians to conduct manual inspections, which require extended periods of work but fail to stop disease outbreaks [10].

Reducing human health hazards and preventing the spread of animal illnesses relies heavily on early diagnosis of LSD. Farmers usually practice traditional methods, which include burning neem leaves and disinfecting their farms, before they seek help from a veterinarian. The visual inspection method which veterinarians use requires manual assessment but creates problems because it takes a long time and leads to errors [11]. When the illness has spread to other cattle, only then does the public learn about it. To detect even subtle changes in cow skin that could be indicative of LSD, researchers are now using state-of-the-art deep learning models in conjunction with convolutional neural networks. The proliferation of LSD cattle picture collections has paved the way for the creation of automated detection methods [12]. Thanks to this technology, farmers and veterinarians can quickly diagnose diseases, which allows for prompt treatment and ultimately reduces the spread of certain diseases [13].

Researchers have successfully deployed deep learning models to identify LSD through their examination of images. The combination of Gaussian filtering and histogram equalization together with convolutional neural networks (CNNs) as feature extraction method led to the achievement of 93% accuracy for cattle image classification into lumpy skin and normal skin categories [14]. Training data accuracy reached 99.01% and testing data accuracy reached 97.87% with the use of pretrained deep learning models InceptionV3, ResNet50V2, and VGG16 in conjunction with a modified CNN system [15]. Problems with developing models that might function well in real-world scenarios arose from the researchers' use of tiny datasets, which hampered the experiments. Even with these impressive accuracy rates, we still don't know how well different deep learning models identify LSD. Evaluating a wider variety of models might help shed light on this mystery. The study proposed the following contributions:

1.1 Contributions of the study

- Utilise a hybrid deep learning architecture to create a system for early diagnosis of lumpy skin condition.
- Introduced an attention-based sparse autoencoder for feature selection
- Design a morphology-aware classifier for improved lesion understanding for classification.
- Achieve stronger and more accurate classifications than top-tier models

1.2 Organization of the Paper

Section 2 presents the relevant research on the current models for detecting lumpy skin diseases. In Section 3, the suggested models' context is laid forth. The study's dataset and planned approach are detailed in Section 4. The findings and discussion are presented in Section 5, and the study ends with future directions in Section 6.

2. Related Work

Because conventional approaches struggle due to a lack of resources and specialist expertise, deep learning algorithms are increasingly crucial for the correct identification of lumpy skin diseases. [16] Created an algorithm that analyses a dataset of instances of Cattle's Lumpy Skin Disease (CLSD) using a 10-layer Convolutional Neural Network (CNN). Use of a colour histogram to extract relevant colour information aids in localising the afflicted regions. Binarization and classification using an Extreme Learning Machine (ELM) classifier provide 90.12% accuracy. The efficacy of the suggested approach is shown by comparing it with current state-of-the-art procedures.

Khaskheli et al.,[17] suggested a new strategy that uses ensemble techniques to identify lumpy skin condition in cattle. A model was developed by the researchers that extracted its characteristics using a Grey Level Co-occurrence Matrix (GLCM). The system was developed and evaluated with 500 images which were obtained from three different districts in Sindh province. Improving picture quality and identifying crucial regions were two goals of the image pre-processing procedures. The model created three categories for cattle based on their physical state and body temperature which included "normal," "high," and "severe" stages. The ensemble technique reached an accuracy level of about 86% according to the results.

Ullah et al.,[18] conducted their study by using 8000 cattle images which they obtained from Kaggle to train their model for optimal infection detection purposes. The ViT architecture was used as our classification approach after data pre-processing methods such as resizing, normalisation, and augmentation were used. Among the remarkable outcomes produced by the model were a 98.5 F1 score, 98.5% recall, 98.5% precision, and 98.12% accuracy. Based on its potential to provide more accurate and precise findings, the study showed that ViT is better than conventional approaches for LSD categorisation.

Shakeel et al., [19] compared the CNN architectures Inception and Xception for identifying patterns and predicting LSD occurrence in animals. After being trained on a massive dataset of tagged pictures, Xception attained an accuracy of 98.8 percent and Inception 94.4 percent. The 4.8% accuracy improvement demonstrates Xception's ability to identify LSD with exactitude which makes it useful for early veterinary diagnosis to enhance animal healthcare operations and decrease the worldwide effects of LSD on cattle populations.

This research study by Sonowal et al., [20] categorizes lumpy skin diseases using a CNN model with hyperparameter optimization. The choice of pre-trained model, which was later customized, resulted in 89.73% accuracy during validation and 80.68% test accuracy. This model increases the rate at which LSDs are identified by farmers and veterinarians. As a last step, a ROC curve yielded an AUC of 0.88.

Raziff et al., [21] studied many deep learning algorithms that automatically detect LSD in pictures of cows. This research compares six different deep learning architectures—CNN-TensorFlow, CNN-SqueezeNet, CNN-Inception, CNN-Xception, Mobile Net, and a CNN built on PyTorch—to more conventional classifiers that rely on support vector machines and support vector libraries. The study used 1,024 images to show that Xception achieved the best accuracy with 90.15%. The results show that automated LSD detection using deep learning models is successful. Deep learning algorithms are successful for automated LSD detection, according to the study.

The existing studies tend to be based on conventional methods which suffer from dependency on handcrafted features and lack the capability to generalize, or on the other hand, on advanced deep learning frameworks like CNN and Vision Transformer models, which require extensive datasets and show low interpretability. Table 1 summarises the research on lumpy skin disease identification that has been conducted thus far.

Table 1: Nomenclature

Symbol / Term	Description
D	Input dataset
X_i	Input image (RGB cattle skin image)
Y_i	Corresponding label (0: Normal, 1: LSD)
N	Total number of samples
$\tilde{X}$	Augmented image using MixUp
$\tilde{y}$	Augmented label
λ	MixUp interpolation coefficient
R	Region of Interest (ROI)
f_{det}	Detection function in LUMPNet
F	Extracted feature vector
d	Dimension of feature vector
Z	Latent feature representation
W_e, b_e	Encoder weights and bias
A	Attention weight vector
Z'	Weighted feature representation
$\hat{F}$	Reconstructed feature vector
L_{FS}	Feature selection loss
F^*	Optimized feature set

Symbol / Term	Description
F_{map}	Reshaped feature map
L	Local features
G	Global features
Z_c	Fused feature representation
$\hat{y}$	Predicted output
L_{CE}	Cross-entropy loss

Table 2: Summary of the Existing Studies on the Lumpy Skin Disease Detection

Reference	Model Type	Image-Based Dataset	Feature Extraction	Feature Selection	Deep Learning	High Accuracy (>95%)	Key Contribution	Limitation
Genemo., [16]	CNN + ELM	✓	✓	✗	✓	✗	Colour histogram + CNN for detection	Moderate accuracy
Khaskheli et al. [17]	GLCM + Ensemble	✓	✓	✗	✗	✗	Texture-based detection	Small dataset
Shroddha et al. [22]	ViT (Mobile-based)	✓	✓	✗	✓	✓	Real-time smartphone detection	Generalization issues
Khotimah et al. [23]	Ensemble DL + CLAHE	✓	✓	✗	✓	✓	Advanced ensemble framework	High computational cost
Ullah et al., [18]	Vision Transformer (ViT)	✓	✓	✗	✓	✓	ViT + mobile app for field-ready accurate detection	Higher compute needs on mobile devices
Sharma et al. [24]	DL + Image Processing	✓	✓	✗	✓	✓	Advanced prediction & severity analysis	Generalizability concerns
Pal et al. [25]	ViT + ConvMixer Ensemble	✓	✓	✗	✓	✓	Ensemble DL system for precise veterinary diagnostics	Dataset dependency; ensemble complexity
Saha [26]	Multiple CNN Architectures	✓	✓	✗	✓	✓	Extensive CNN comparison	Computationally intensive training
Alzubi [27]	Advanced CNN	✓	✓	✗	✓	✗	Robust CNN approach for LSD detection	Black-box interpretability issues
Saqib et al. [28]	MobileNet V2 + RMSProp	✓	✓	✗	✓	✓	Lightweight optimized model	Performance may vary with new datasets
Kumar et al. [29]	Deep Learning	✓	✓	✗	✓	✗	DL advancement in veterinary healthcare	Book chapter; fewer technical specifics
Reddy et al. [30]	CNN + ELM	✓	✓	✗	✓	✓	High-risk zone identification & segmentation	Zone-focused rather than individual diagnosis

2.1 Research Gap

The use of ML and DL approaches to diagnose lumpy skin diseases has come a long way, but there are still several crucial challenges that need to be resolved. Existing research studies depend on two main approaches which include traditional machine learning systems that use user-defined features and have restricted capabilities and deep learning systems that require extensive data and high processing power which include CNNs and Vision Transformers. The various methods use effective feature extraction techniques which include CNN and GLCM and ViT yet they fail to implement feature selection processes for LSD, which results in duplicate data and unneeded content that decreases model performance and understanding ability. Moreover, the existing models do not address the issue of morphology-aware learning since they are unable to analyse both local and global features of lesions at the same time. In addition, most deep learning approaches have low interpretability and poor robustness when applied to heterogeneous or field data (low-quality images captured via smartphones). Hybrid models that include data enhancement, feature extraction, feature selection, as well as morphology-aware classification are therefore required.

Therefore, there is a need of a novel hybrid framework that combines effective data augmentation techniques with area-centric feature extraction methods and attention-based feature selection strategies and morphology-aware classification systems to improve precision and decrease unnecessary elements and enhance understanding and maintain reliable results in various real-world situations.

3. Methodology

This research develops a combined deep learning system which detects Lumpy Skin Disease (LSD) through its use of data augmentation and deep feature extraction together with its attention feature selection method and its morphology-based classification system. The pipeline consists of four linked processes which include (i) MixUp-based data augmentation and (ii) LUMPNet-based feature extraction and (iii) Attention-Based Sparse Autoencoder (AB-SAE) feature selection and (iv) MADC-based final classification. The system at each stage of its operation establishes better system strength through decreased system weight and improved ability to distinguish between different conditions which leads to precise disease identification.

3.1 Dataset Description

The Lumpy Skin Images Dataset provided the data used in this investigation [31], which is available from the following website: https://data.mendeley.com/datasets/w36hpf86j2/1.

The research also compares the suggested model to other datasets from previous studies that deal with lumpy skin condition. The datasets are Cow lumpy disease dataset [32], available from the following website: https://www.kaggle.com/datasets/shivamagarwal29/cow-lumpy-disease-dataset. Cattle diseases datasets [33], available from the following website: https://www.kaggle.com/datasets/devang03mgr/cattle-diseases-datasets. Table 3 provides a description of the datasets.

Table 3: Description of the Datasets

Datasets	Type	No. of Figures	Task	Classes
Mendeley LSD Image Dataset (Your Dataset)	Image	1024	Binary	Normal, LSD
Cow Lumpy Disease Dataset	Image	939	Binary	Normal, LSD
Cattle Diseases Dataset	Image	3424	Multi-class	Normal, LSD, other diseases

Table 4: Sample Images from the Dataset

Classes	Normal	Lumpy Skin

1		
2		
3		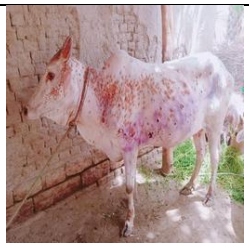

3.2 Dataset Representation and Preprocessing

Let the input dataset be represented as:

$$\mathcal{D} = \{(X_i, y_i)\}_{i=1}^{N} \quad (1)$$

where $X_i \in \mathbb{R}^{H\times W\times 3}$denotes the i^{th}RGB image of cattle skin with height H, width W, and three-color channels, and $y_i \in \{0,1\}$ stands for the matching category label, where 0 denotes a healthy sample and 1 denotes a sample infected with LSD2. As a whole, the dataset has N samples.

To guarantee uniform input distribution, all photos are normalised and scaled to a set resolution before to training. Training is stabilised and deep learning architecture compatibility is guaranteed by this normalisation.

3.3 Data Augmentation using MixUp

The MixUp augmentation approach is used to overcome dataset restrictions and enhance generalisation. In order to train the algorithm to make more refined decisions, MixUp creates synthetic samples by combining picture and label pairings.
The augmented image $\tilde{X}$is computed as:

$$\tilde{X} = \lambda X_i + (1-\lambda)X_j \quad (2)$$

and the corresponding label is:

$$\tilde{y} = \lambda y_i + (1-\lambda)y_j \quad (3)$$

Where X_i and X_j are two input photographs that were chosen at random, and the labels for each image are y_i and y_j. The mixing ratio $\lambda \in [0,1]$ manages the impact of every sample and is selected using a Beta distribution:

$$\lambda \sim \text{Beta}(\alpha, \alpha) \quad (4)$$

Here, α lower values of α generate samples that are closer to the original pictures, whilst higher values provide more blended samples; this hyperparameter controls the intensity of interpolation. Understanding that any procedure which could sum up different data variations would actually reinforce the subsequent stability.

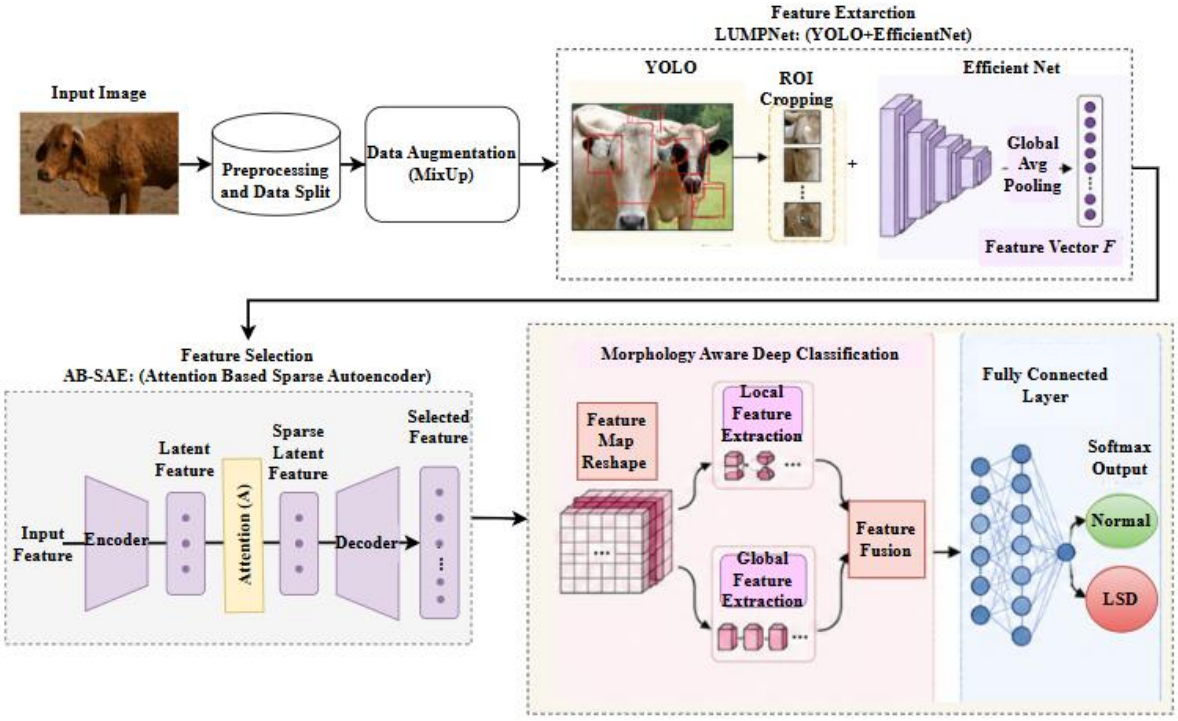

Figure 1: Architecture of the Proposed Study

3.4 Feature Extraction using LUMPNet

LUMPNet performs feature extraction after data addition because its system combines object detection with deep feature learning. The project currently works on developing an accurate model which will identify lesion locations by removing all background elements and extracting essential distinguishing features.
Given an augmented image$\tilde{X}$, the first thing the model does is localize the region of interest (ROI), which may probably contain lesions:

Where $f_{\text{YOLO}}(\cdot)$The detection function needs to use the detection function together with R which represents the extracted ROI. The current step restricts feature extraction to function only in disease-related areas of research.

To generate a deep feature representation, the ROI is followed by an EfficientNet backbone:

$$F = f_{\text{EffNet}}(R) \quad (6)$$

Where $F \in \mathbb{R}^d$ The high-dimensional aggregated feature vector consists of dimensions that exactly match the value of d. These attributes usually account for texture, color, and spatial information related to brain lesions.

Feature Selection using Attention-Based Sparse Autoencoder

An Attention-Based Sparse Autoencoder (AB-SAE) is used to preserve just the most useful features and eliminate duplication. This module performs dimensionality reduction while assigning importance weights to features.

Encoder Transformation

Encoder creates a lower-dimensional latent space from the high-dimensional feature vector F:

$$Z = \sigma(W_e F + b_e) \quad (7)$$

Where $Z \in \mathbb{R}^k$is the latent representation with reduced dimensionality $k(k < d)$, $W_e \in \mathbb{R}^{k \times d}$is the encoder weight matrix, $b_e \in \mathbb{R}^k$is the bias vector, and $\sigma(\cdot)$implies, therefore, the requirement for a non-linear activation function such as ReLU.

Attention-Based Feature Weighting

I look forward to finding the right side-feature of the object using the saliency model:

$$A = \text{Softmax}(W_a Z) \quad (8)$$

$$Z' = Z \odot A \quad (9)$$

Where $A \in \mathbb{R}^k$represents the attention weight vector, W_a is the attention parameter matrix, and $\odot$ denotes element-wise multiplication. The vector Z' click for your desired features, having higher relevance on the attention weights.

Decoder Reconstruction

The original feature vector input and the decoder are presented during the learning process:

$$\hat{F} = \sigma(W_d Z' + b_d) \quad (10)$$

Where $\hat{F} \in \mathbb{R}^d$the reconstructed feature is vector, $W_d$and b_d the parameters which decode the system operate through its decoding parameters. The "reconstruction" process enables selected features to maintain sufficient informational content.

Feature Selection Loss Function

A composite loss function is used to train the autoencoder:

$$\mathcal{L}_{FS} = || F - \hat{F} ||_2^2 + \lambda_1 || A ||_1 \quad (11)$$

Where $|| F - \hat{F} ||_2^2$ The only-BOW loss refers to loss (reconstruction loss) across any replacement of the original features with the reconstructed features, $|| A ||_1$is the L1 a regularization term that enforces sparsity on the weights λ_1 this very first version promotes harmony between the two aforementioned conflicting tendencies?

The sign that was ultimately chosen for the identifier was called a sign:

$$F^* = Z' \quad (12)$$

3.5 Classification using MADC

The optimized feature set F^* The Morphology-Aware Deep Classifier (MADC) receives its input data which was designed to achieve precise Lumpy Skin Disease (LSD) lesion classification through its system that detects both regional texture elements and complete structural design patterns.

Feature Reshaping

In order for the feature to be spatially learned, transforming from the feature vector onto a tensor would become rather important:

$$F_{map} \in \mathbb{R}^{h \times w \times c} \quad (13)$$

c, w, and h represent the channel dimension, the spatial height, and the breadth, respectively.

Local and Global Feature Extraction

Convolution operations of smaller receptive fields are used to get local features:

$$L = f_{local}(F_{map}) \quad (14)$$

Spreading attention around the finer textures of the lesions that lash around edge-level details.

Morphology following worldly outlook is capturing through large receptive fields combined with pooling tasks:

$$G = f_{global}(F_{map}) \quad (15)$$

with the use of ", data was collected with specificity in respect to the structural characteristics of the lesions and their distribution.

3.6 Feature Fusion and Prediction

The first step is deciding the particular class to which one would like to contribute. In our case L and G are particularly relevant, but many others can get involved in the design:

$$Z_c = \gamma L + (1 - \gamma)G \quad (16)$$

Where $\gamma \in [0,1]$controls the contribution of local and global features.

The final prediction is obtained using:

$$\hat{y} = \text{Softmax}(W_c h + b_c) \quad (17)$$

Where, $\hat{y}$ is the predicted probability vector, W_h, W_c and b_h, b_c parameters that can be learned, $\phi(\cdot)$it intends to function as an activation function which is non-linear, just like ReLU.

3.7 Model Training

A combined loss is used to train the whole model:

$$L = L_{CE} + \lambda_2 L_{FS} \quad (18)$$

Here we define the cross-entropy loss as:

$$L_{CE} = -\frac{1}{N}\sum_{n=1}^{N} \sum_{i=1}^{C} y_{n,i} \log(\hat{y}_{n,i}) \quad (19)$$

Where, CE denotes the cross entropy, N is equal to how many samples, C how many different types, $y_{n,i}$ represents the truth label $\hat{y}_{n,i}$ is the likelihood that is anticipated.

3.8 Performance Evaluation

The researchers assessed system stability by testing it with three different datasets and their corresponding dataset. The evaluation metrics are given below:

Accuracy: One of the most important metrics for measuring a classification model's performance is its accuracy. What this number represents is the percentage of correct predictions made by the model as a percentage of all forecasts.

$$Accuracy = \frac{TP+TN}{TP+TN+FP+FN} \quad (20)$$

Precision: It measures the accuracy rate of the model's positive predictions. In fields where the potential consequences of incorrect diagnoses might be devastating, such as medical diagnostics, this approach is useful because of the high cost of false positives.

$$Precision = \frac{TP}{TP+FP} \quad (21)$$

Recall: Recall, often called sensitivity, is the number of positive cases that the model correctly identified. In cases when the cost of a false negative is higher than that of a false positive, this is of the utmost importance.

$$Recall = \frac{TP}{TP+FN} \quad (22)$$

F1-Score: The F1 Score is a harmonic average of the recall and accuracy. Since it combines accuracy and recall into one figure, it helps to strike a balance between the two. The model's performance meets both requirements when the F1 score is high. Within this range, you will find the value 1. Superior accuracy is achieved with lower recall and improved precision, but a large proportion of instances are missed. An improved performance is indicated by a higher F1 score. This might be expressed as:

$$F1\ Score = 2 \times \frac{Precision \times Recall}{Precision+Recall} \quad (23)$$

The numbers TP, TN, FP, and FN stand for the number of true positives, true negatives, false positives, and false negatives, respectively. The models were trained and assessed using the same fixed 80:20 train-test split. Construction of confusion matrices and evaluation metrics was done with the same test set, ensuring fair viewing in performance comparison.

ROC-AUC: The AUC score which calculates the area under the ROC curve serves as a reliable method to evaluate how well a model performs its prediction tasks. The method shows the likelihood that two randomly chosen instances which include one positive instance and one negative instance will receive different ratings.

The proposed framework establishes a multi-step system which LUMPNet uses for detection-based feature extraction and the system applies an attention-driven sparse autoencoder to select features before it uses the LSDD morphology-based classification system. The approach successfully reduces feature replication while preserving lesion structure and enhancing classification performance which addresses critical research deficiencies present in current academic studies. The process of feature extraction and selection helps to decrease redundancy while producing more distinct features, but it fails to directly identify the structural elements that define Lumpy Skin Disease lesions. The structural patterns found in LSD identification include nodular formations and spatial distribution which conventional classifiers cannot successfully model. The system includes a morphology-based deep learning classifier which processes local texture information and global structural dependencies to produce precise clinical predictions.

Table 5: Algorithm of the Proposed Methodology

Algorithm: M-LSA-Net LSD Detection
Input: Dataset D = {(Xi, yi)}, i = 1 to N
Output: Predicted label ŷ
1: Initialize model parameters θ
2: Preprocess dataset:
3: Resize images and normalize inputs
4: Split dataset into training and testing sets

Algorithm: M-LSA-Net LSD Detection
5: for each training iteration do
6: // Step 1: MixUp Data Augmentation
7: Select two random samples (Xi, yi) and (Xj, yj)
8: Generate mixing coefficient λ using Eq. (4)
9: Create augmented sample $\tilde{X}$ using Eq. (2)
10: Generate augmented label $\tilde{y}$ using Eq. (3)
11: // Step 2: Region-Focused Feature Extraction (LUMPNet)
12: Detect region of interest R using Eq. (5)
13: Extract feature vector F using Eq. (6)
14: // Step 3: Feature Selection (AB-SAE)
15: Encode features to latent space Z using Eq. (7)
16: Compute attention weights A using Eq. (8)
17: Apply attention to obtain Z′ using Eq. (9)
18: Reconstruct features $\hat{F}$ using Eq. (10)
19: Compute feature selection loss L_FS using Eq. (11)
20: Obtain optimized features F* using Eq. (12)
21: // Step 4: Morphology-Aware Classification (MADC)
22: Reshape features into feature map F_map using Eq. (13)
23: Extract local features L using Eq. (14)
24: Extract global features G using Eq. (15)
25: // Step 5: Feature Fusion and Prediction
26: Fuse features Zc using Eq. (16)
27: Compute predicted output $\hat{y}$ using Eq. (17)
28: // Step 6: Optimization
29: Compute classification loss L_CE using Eq. (19)
30: Compute total loss L using Eq. (18)
31: Update model parameters θ using backpropagation
32: end for
33: Return final predicted label $\hat{y}$

Table 5 Algorithm of the Proposed Methodology

4. Results and Discussion

To provide a fair comparison across all models, the proposed M-LSA-Net model was tested on the Lumpy Skin Images Dataset utilising an 80:20 train-test split. Accuracy, Precision, Recall, F1-score, and ROC-AUC were some of the common measures used to evaluate performance after pre-processing (resizing and normalising all pictures to 256×256).

4.1 Results of Proposed Model

Tabulated in Table 2 is the suggested model's performance evaluation on the test dataset.

Table 6: Performance of Proposed M-LSA-Net Model

Metric	**Value**
Accuracy	0.9871
Precision	0.9868

Metric	Value
Recall	0.9871
F1-Score	0.9869
ROC-AUC	0.9978

With a 98.71% success rate, the suggested model clearly has excellent classification skills when it comes to differentiating between normal and lumpy skin. This model consistently minimises both false positives and false negatives, which is crucial in medical diagnostic situations, as shown by the balanced values of recall and accuracy. The model's capacity to efficiently distinguish between the two classes across various threshold settings is further supported by the ROC-AUC score of 0.9978.

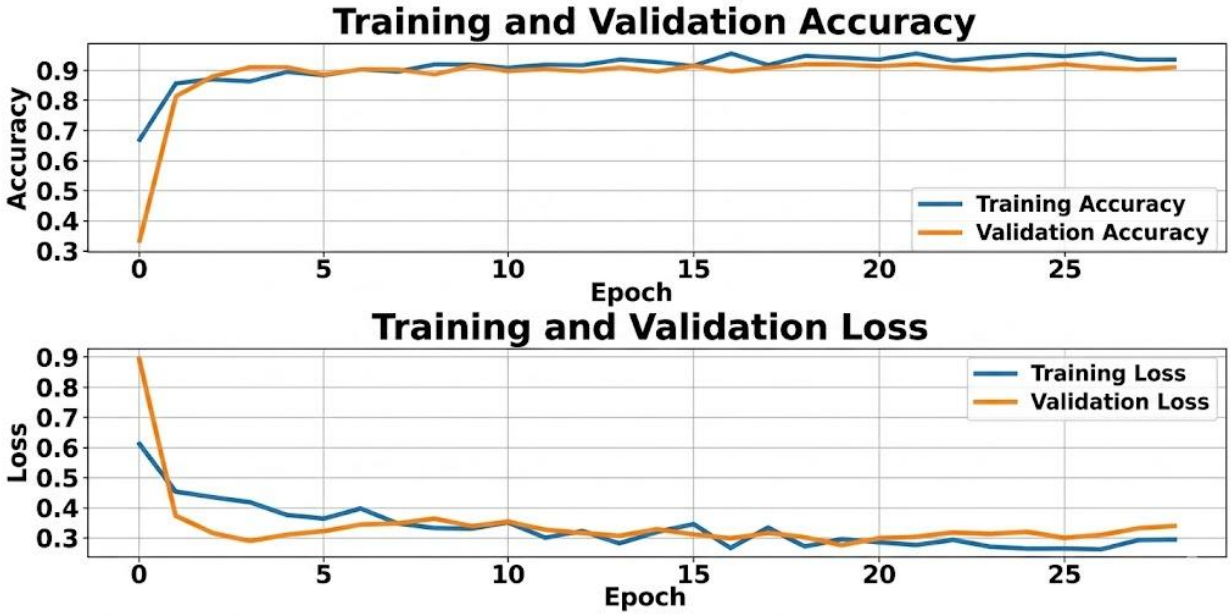

Figure 2: Accuracy and Loss of Training and Validation

XX

Figure 2: shows the training as well as validation curves, which show that the suggested model accomplishes consistent performance by means of extensive learning capabilities. The training and validation losses show an initial sharp decrease because of effective learning during the first training period which results in validation loss dropping from a high value of approximately 0.90 to less than 0.35 within several training periods. The training process leads to both losses reaching stable points which exhibit minor changes that result in values between 0.28 and 0.33 which demonstrates successful optimization that avoids major performance drops. The accuracy curves display an ongoing improvement which leads to training accuracy growing from 67% to 94-95% and validation accuracy increasing from 32% to 90-91%. The model demonstrates strong generalization abilities because training and validation accuracy closely match each other and there exists only a slight difference in the loss curves. The M-LSA-Net model shows reliable convergence stable performance and equal learning progress according to the training and validation data.

4.2 Comparative Analysis with Existing Studies

In order to confirm that the suggested method works, M-LSA-Net was compared to three popular baseline models:

Table 7: Comparative Analysis with Existing Studies

Model	Accuracy	Precision	Recall	F1-Score	AUC
CoAtNet	0.9578	0.9562	0.9550	0.9556	0.9690
SwinT V2	0.9635	0.9620	0.9608	0.9614	0.9738

Model	Accuracy	Precision	Recall	F1-Score	AUC
Max-ViT	0.9782	0.9668	0.9655	0.9661	0.9795
M-LSA-Net (Proposed)	0.9871	0.9868	0.9871	0.9869	0.9978

Table 7: shows how the proposed M-LSA-Net performed in comparison to other deep learning models developed recently for picture categorisation tasks. Among the baseline models, CoAtNet achieves an accuracy of 95.78%, followed by Swin Transformer V2 with 96.35% and Max-ViT with 96.82%, indicating the strong capability of hybrid and transformer-based architectures in capturing complex visual patterns. With an accuracy of 98.71%, higher precision of 98.68%, recall of 98.71%, F1-score of 98.69%, and AUC of 98.78%, the suggested M-LSA-Net considerably surpasses all comparable models. The efficacy of the suggested framework in improving classification performance is shown by this substantial improvement.

4.3 Confusion Matrix

All four of these systems are laid forth in the Confusion Matrix M-LSA-Net Max-ViT SwinT V2 and CoAtNet perform in classifying data from the binary classification dataset which distinguishes Normal from LSD.

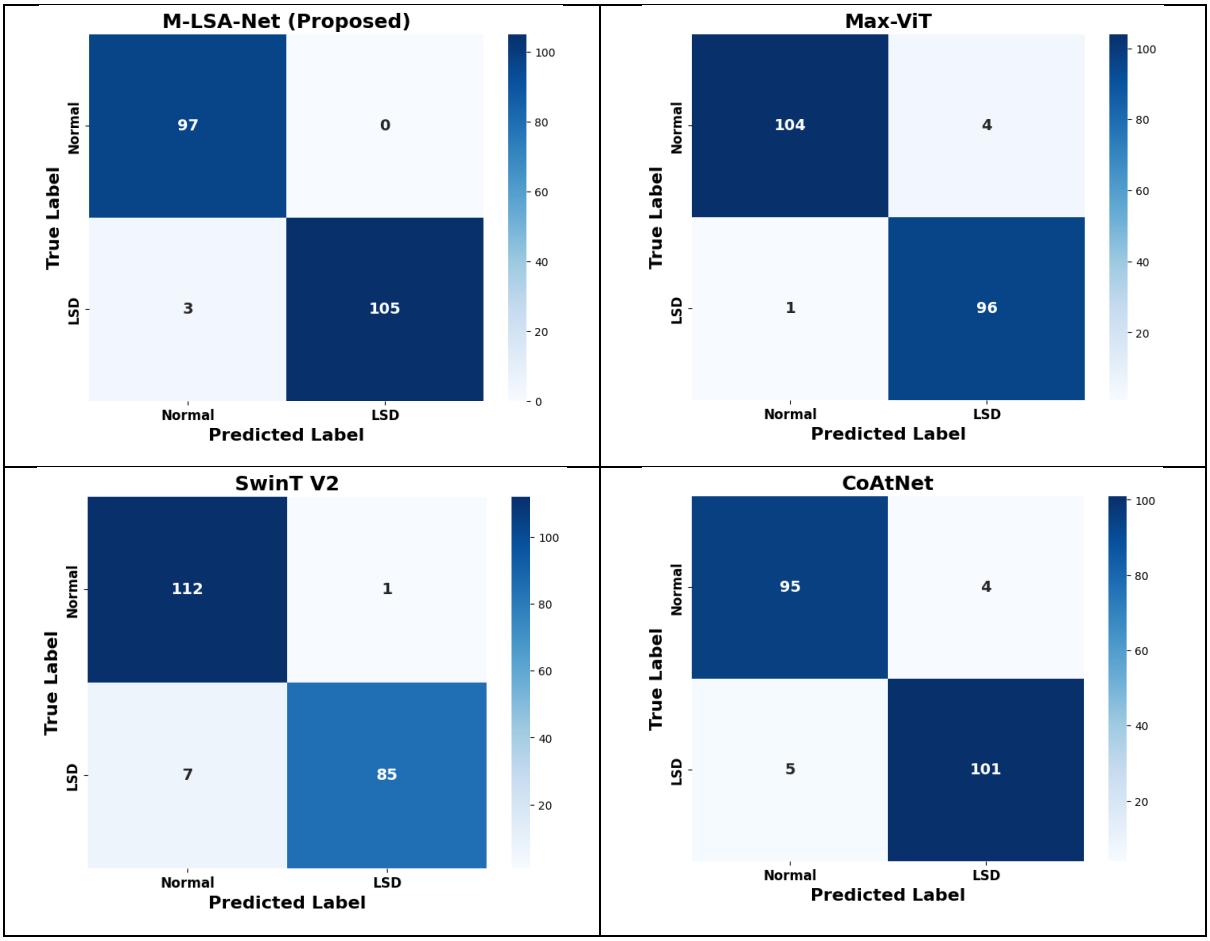

Figure 3: Confusion matrix of the Proposed Model and Existing Models

Overall, the M-LSA-Net (Proposed) model reaches 98.53% accuracy, which is its greatest prediction accuracy, thanks to its four architectural designs. The system shows perfect accuracy for "Normal" class detection because it has not made any False Positive errors. The system effectively detects 105 of 108 LSD class cases and makes 3 False Negative errors. The proposed architecture demonstrates its power to extract features and learn discriminative patterns because it maintains a very low error rate with this specific dataset. The Max-ViT model demonstrates strong

performance which achieves an accuracy rate of 97.56%. The model demonstrates a strong ability to differentiate between the two classes, correctly classifying 200 out of 205 samples. The system shows a minor trade-off between classification accuracy and classification bias because it misclassified four Normal instances as LSD and one LSD instance as Normal which demonstrates a tendency to classify cases as Normal rather than LSD cases. SwinT V2 is more prone to classification errors, especially when it comes to the "LSD" category. This model had an accuracy rate of about 96.10%. It has a very strong performance in recognizing the Normal category (with 112 true positives), yet having a higher number of 7 mistakes in the LSD category suggests that this model finds it difficult to represent unique variances in the LSD data set. CoAtNet has the worst accuracy of all models in this list, which is about 95.61%. The model has a rather balanced error distribution, with 4 cases where Normal samples were classified as LSD and 5 instances where LSD samples were classified as Normal. Although the accuracy score is stable, the greater number of errors indicates that CoAtNet's features are slightly less suitable for classification tasks than those of the best-performing M-LSA-Net.

4.4 Comparison with Existing Studies

Table 8: Proposed Model Performance Comparison with Existing Studies

Reference	Model	Accuracy	Precision	Recall	F1-Score
Sharma et al., 2026 [24]	Hybrid CNN	97.77	98.4	96.3	97.3
Reddy et al., 2025 [30]	ELM	96	95.8	96.2	96
Khaskheli et al., 2025 [17]	Ensemble Technique	86	86	86	86.01
Jeevan & Veena, [34]	Custom CNN model	93	93.8	91.7	92.7
Saqib et al., 2024 [28]	MobileNetV2+RMSprop	95	95	95	95
Velugoti et al., 2024 [35]	DenseNet169	95.10	95.10	95.10	95.10
This Work	M-LSA-Net	0.9871	0.9868	0.9871	0.9869

The table 8 shows results which compare the proposed M-LSA-Net model with the existing methods for Lumpy Skin Disease detection. The earlier studies show a wide variation in performance depending on the model complexity and learning strategy. The hybrid CNN model by Sharma et al. (2026) demonstrates strong performance which results in 97.77% accuracy and high precision while Reddy et al. (2025) using an ELM-based approach reports a balanced accuracy of 96%. The ensemble technique used by Khaskheli et al. (2025) achieves lower results which reach 86% because the method fails to properly represent features. The custom CNN developed by Jeevan and Veena and the MobileNetV2-based optimization system created by Saqib et al. show performance results that range from 92% to 95% according to their respective deep learning methods. The results for DenseNet169 remain steady at 95.10% throughout all tests. The M-LSA-Net system outperforms all competing systems because it achieves an accuracy rate of 98.71% while delivering better precision results at 98.68% and better recall results at 98.71% and better F1-score results at 98.69%.

The proposed system improves performance because it captures distinguishing characteristics which lead to correct identification of different things. The performance gain can be attributed to the integration of region-focused feature extraction, attention-based sparse feature selection, and morphology-aware classification, which together enhance both local and global feature learning while reducing redundancy. The results demonstrate that M-LSA-Net exists as a superior and dependable detection solution for LSD detection when compared to existing detection models.

4.5 Ablation Study

By progressively adding modules to the baseline model, an ablation study was conducted to validate the significance of each module in the proposed system design. Metadata such as F1-score, Accuracy, Precision, and Recall formed the basis of these assessments.

Table 9: Ablation Study

Configuration	Accuracy (%)
LUMPNet only	97.52
+ MixUp	98.03
+ Feature Selection (AB-SAE)	98.42

Configuration	Accuracy (%)
+ LSDD (Full Model: M-LSA-Net)	98.71

The ablation study shows that accuracy increases from 97.52% to 98.71% when additional modules are added. MixUp implementation improves generalization results while attention-based feature selection methods identify actual necessary features. The morphology-driven classifier achieves its best results because it can detect specific structural patterns that are needed to identify lesions.

4.6 Dataset Comparison

The research tested the framework on two publicly available datasets—the Cow Lumpy Disease Dataset and the Cattle Diseases Dataset—which were used to evaluate the system's capacity to perform across different situations. The two datasets serve as appropriate evaluation materials because they contain different levels of class diversity and operational complexity and authentic world situation variability.

Table 10: Dataset Comparison with Proposed Model

Dataset	Accuracy (%)	Precision	Recall	F1-score
Mendeley LSD Image Dataset (This study Dataset)	98.71	0.9868	0.9871	0.9869
Cow Lumpy Disease Dataset	98.21	0.9825	0.9832	0.9828
Cattle Diseases Dataset	97.84	0.9772	0.9785	0.9778

The table 8 shows the M-LSA-Net model across different datasets to verify its performance and ability to generalize across different data types. The model achieves its highest accuracy score of 98.71% on the Mendeley Lumpy Skin Disease dataset according to Table X which shows its precision score at 0.9868 and its recall score at 0.9871 and it's F1-score at 0.9869. The dataset delivers superior results because it maintains a clean structure which enables clear detection of lesion patterns and maintains equal distribution of different classes throughout the dataset. With precision values of 0.9825, recall values of 0.9832, and F1-score values of 0.9828, the model achieves an accuracy of 98.21% on the Cow Lumpy Disease Dataset. The system experiences a minor performance drop because of two factors: the system faces more background changes and the image conditions face less control. The system shows 97.84% accuracy on the Cattle Diseases Dataset which tests its ability to classify multiple categories of diseases that share similar visual characteristics. The performance decline occurs because the system experiences both higher internal similarity among its classes and increased difficulty in distinguishing different classes. Its capacity to manage binary and multi-class illness classification jobs is shown by the model's consistent excellent performance across all datasets.

4.7 Statistical Significance

Table 11: Statistical Significance of the Proposed Model

Model	Accuracy	Precision	Recall	F1-score	p-value (vs Proposed)	Significance
CoAtNet	0.9578 ± 0.009	0.9562 ± 0.010	0.9550 ± 0.010	0.9556 ± 0.010	0.001	Significant
SwinT V2	0.9635 ± 0.008	0.9620 ± 0.009	0.9608 ± 0.009	0.9614 ± 0.009	0.001	Significant
Max-ViT	0.9782 ± 0.006	0.9668 ± 0.007	0.9655 ± 0.007	0.9661 ± 0.007	0.012	Significant
M-LSA-Net (Proposed)	0.9871 ± 0.003	0.9868 ± 0.002	0.9871 ± 0.002	0.9869 ± 0.002	<0.01	—

The table 9 shows the performance comparison between M-LSA-Net and CoAtNet, SwinT V2, and Max-ViT using k-fold cross-validation results which present mean values together with their standard deviations. The suggested model outperforms all other models because it achieves superior accuracy three metrics which include precision and recall and F1-score performance, and it maintains the least variability which demonstrates its ability to operate with consistent performance. The statistical analysis demonstrated that CoAtNet and SwinT V2 improvements reached

high significance levels ($p < 0.001$) while the Max-ViT improvement showed statistical significance at ($p = 0.012$). The proposed model shows both effective performance and excellent operational stability according to its results.

5. Discussion

M-LSA-Net achieves better performance because its system works together with three components which include MixUp-based data augmentation and region-of-interest feature extraction and attention-based sparse feature selection and morphology-aware classification. The Swin Transformer V2 and Max-ViT models use their attention systems to learn global context understanding but they need more capacity to concentrate on particular lesion regions and require additional abilities to select features through their systems. M-LSA-Net achieves better feature representation because it simultaneously examines local texture details and global structural patterns that exist in lesions. The accuracy improvement over Max-ViT which represents the best-performing baseline reaches 1.89% but this difference holds important value for medical image classification because even minor changes result in better diagnostic accuracy and decision-making abilities. In comparison to current state-of-the-art models, the findings show that the suggested method outperforms them in terms of generalizability, classification efficacy, and robustness.

6. Conclusion

Presenting M-LSA-Net, a hybrid deep learning-based approach for fast and effective image processing-based lumpy skin disease detection in cattle. In the proposed architecture, there is an effective use of different modules in the network which includes Mixup, LUMPNet for Region-based feature extraction, Feature Selection with Attention and Morphology-based classification. With an impressive f-score of 98.71% and very high accuracy, precision, and recall, experimental data show that M-LSA-Net outperforms the current deep learning methods. Not only the model gives high accuracy but has been shown to be generalized on various datasets. The ablation experiment performed shows that the importance of every module in the network and that the modules like feature selection and morphology-based learning contribute significantly to the improvement of classification.

The study demonstrates strong performance but has specific limitations which arise from its reliance on image quality and its requirement for additional testing on extensive authentic datasets that contain various environmental conditions. The research will develop mobile applications through the implementation of reduced model versions which will use explainable artificial intelligence methods to enhance user understanding and test the system using data collected under diverse environmental conditions. In conclusion, the presented M-LSA-Net is an efficient approach for early LSD detection.

$$R = f_{\text{YOLO}}(\tilde{X}) \tag{5}$$

Reference

1. K. Yao and S. Wang, “Understanding the research advances on lumpy skin disease : A comprehensive literature review of experimental evidence,” no. November, 2022, doi: 10.3389/fmicb.2022.1065894.
2. A. Mazloum, A. Van Schalkwyk, S. Babiuk, E. Venter, D. B. Wallace, and A. Sprygin, “Lumpy skin disease : history, current understanding and research gaps in the context of recent geographic expansion,” no. November, 2023, doi: 10.3389/fmicb.2023.1266759.
3. F. Namazi and A. Khodakaram Tafti, “Lumpy skin disease, an emerging transboundary viral disease: A review,” Vet. Med. Sci., vol. 7, no. 3, pp. 888–896, May 2021, doi: https://doi.org/10.1002/vms3.434.
4. T. Gupta, V. Patial, D. Bali, S. Angaria, M. Sharma, and R. Chahota, “A review: Lumpy skin disease and its emergence in India,” Vet. Res. Commun., vol. 44, no. 3, pp. 111–118, 2020, doi: 10.1007/s11259-020-09780-1.
5. A. Kaur and K. Singh, “Evaluating Machine Learning Methods Voting System for Predicting the Occurrence of Lumpy Skin Condition,” vol. 15, no. 3, 2023, doi: 10.18090/samriddhi.v15i03.07.
6. D. F. Dofadar, H. Abdullah, R. H. Khan, R. Rahman, and S. Ahmed, “A Comparative Analysis of Lumpy Skin Disease Prediction Through Machine Learning Approaches”.
7. Karthikevan, D. M. V, and M. S. R, “Lumpy Skin Disease Prediction Using Machine Learning,” in 2024 2nd International Conference on Intelligent Data Communication Technologies and Internet of Things (IDCIoT), 2024, pp. 887–895. doi: 10.1109/IDCIoT59759.2024.10467939.
8. A. Gupta, D. Singh, R. Gupta, and V. Tripathi, “Revolutionizing Cattle Health: A Machine Learning Approach to Efficiently Predict Lumpy Disease in Cows,” in 2023 4th IEEE Global Conference for Advancement in Technology (GCAT), 2023, pp. 1–6. doi: 10.1109/GCAT59970.2023.10353420.
9. E. Chandralekha, J. V.M, T. Anitha, V. Deepa, V. Usha, and S. R., “Predicting and Analysing Lumpy Skin Disease Using Ensemble of Machine Learning Models,” in 2023 Global Conference on Information Technologies and Communications (GCITC), 2023, pp. 1–6. doi: 10.1109/GCITC60406.2023.10425950.

10. M. D. N. Begum, J. Prashanthi, K. Priyanka, and J. Supraja, “Deep Learning Mechanisms For Intelligent Lumpy Disease Detection For Enhancing Rural Livelihoods, Sustainable Farming, And Farmer Support System,” vol. 13, no. 5, pp. 904–919, 2025.
11. K. Tikarya, Y. V Jain, and D. Bhise, “A review: Cattle Breed and Skin Disease Identification Using Deep Learning,” in 2023 International Conference on Computing, Communication, and Intelligent Systems (ICCCIS), 2023, pp. 835–842. doi: 10.1109/ICCCIS60361.2023.10425776.
12. C. Senthilkumar, S. C, G. Vadivu, and S. Neethirajan, “Early Detection of Lumpy Skin Disease in Cattle Using Deep Learning—A Comparative Analysis of Pretrained Models,” 2024. doi: 10.3390/vetsci11100510.
13. D. Dommeti, S. R. Nallapati, C. Lokesh, S. P. Bhuvanesh, V. V. P. Padyala, and P. V. V. S. Srinivas, “Deep Learning Based Lumpy Skin Disease (LSD) Detection,” in 2023 3rd International Conference on Smart Data Intelligence (ICSMDI), 2023, pp. 457–465. doi: 10.1109/ICSMDI57622.2023.00087.
14. A. Chinta, G. K. Vathumilli, S. S. Dhara, and L. P. Uriti, “Lumpy Skin Disease Detection in Cows Using Resnet-50,” in 2023 International Conference on Ambient Intelligence, Knowledge Informatics and Industrial Electronics (AIKIIE), 2023, pp. 1–6. doi: 10.1109/AIKIIE60097.2023.10389970.
15. J. P. Singh, D. Ghosh, and J. Singh, “A Novel Deep Learning and Image Processing Based Technique for Lumpy Skin Disease Detection,” in 2024 International Conference on Advancements in Smart, Secure and Intelligent Computing (ASSIC), 2024, pp. 1–5. doi: 10.1109/ASSIC60049.2024.10507897.
16. M. Genemo, “Detecting High-risk Area for Lumpy Skin Disease in Cattle Using Deep Learning Feature,” Adv. Artif. Intell. Res., vol. 3, pp. 27–35, Feb. 2023, doi: 10.54569/aair.1164731.
17. S. A. Khaskheli, M. Y. Koondhar, Z. A. Maher, G. B. Khaskheli, and A. A. Khaskheli, “A Model for Early Detection of Lumpy Skin Disease in Cattle Using Ensemble Technique,” vol. 57, no. 4, pp. 1797–1801, 2025.
18. A. Ullah et al., “A vision transformer model-integrated mobile application for early and accurate detection of lumpy skin disease in cattle,” Sci. Rep., vol. 16, no. 1, p. 683, 2025, doi: 10.1038/s41598-025-30259-z.
19. M. Z. Shakeel et al., “A Deep Learning Tool for Early Detection and Control of Lumpy Skin Disease Using Convolutional Neural Networks,” vol. 07, no. 02, 2024.
20. G. Sonowal, S. G. Singh, P. Bairagi, D. Das, M. Iltimas, and G. Gurbanova, “COMPREHENSIVE EVALUATION AND PERFORMANCE ANALYSIS OF A DEEP LEARNING MODEL WITH HYPERPARAMETER TUNING FOR LUMPY SKIN DISEASE CLASSIFICATION IN DAIRY COWS,” vol. 20, no. 7, pp. 58–65, 2025.
21. A. R. A. Raziff, M. S. M. Pozi, R. Mohamed, and A. A. Samsudin, “A Comparative Study of Deep Learning Models for Automated Detection of Lumpy Skin Disease (LSD) in Cattle,” in 2025 10th International Conference on Information and Communication Technology for the Muslim World (ICT4M), 2025, pp. 1–6. doi: 10.1109/ICT4M68001.2025.11363489.
22. S. I. Shroddha et al., “SmartFarming: Lumpy Skin Disease Detection from Smartphone-captured Cattle Images using Transformer Model,” in 2024 27th International Conference on Computer and Information Technology (ICCIT), 2024, pp. 1040–1045. doi: 10.1109/ICCIT64611.2024.11022547.
23. B. K. Khotimah, B. D. Satoto, Y. D. Pramudita, D. A. Dewi, and F. A’yuni, “A Robust Ensemble Deep Learning Model for Lumpy Skin Disease Identification,” Eng. Technol. Appl. Sci. Res., vol. 16, no. 1, pp. 31285–31293, Feb. 2026, doi: 10.48084/etasr.14823.
24. S. Sharma et al., “ADVANCED PREDICTION MODEL FOR EARLY DETECTION OF LUMPY SKIN DISEASE USING LEARNING AND IMAGE PROCESSING,” J. Mech. Contin. Math. Sci., vol. 21, pp. 26–50, 2026, doi: 10.26782/jmcms.2026.01.00002.
25. M. Pal et al., “Implementation of a Deep Learning System for Detection and Classification of Lumpy Skin Disease in Cattle: Enhancing Precision and Efficiency in Veterinary Diagnostics,” Vet. Med. Sci., vol. 11, no. 6, p. e70664, Nov. 2025, doi: 10.1002/vms3.70664.
26. D. K. Saha, “An extensive investigation of convolutional neural network designs for the diagnosis of lumpy skin disease in dairy cows,” Heliyon, vol. 10, no. 14, p. e34242, 2024, doi: 10.1016/j.heliyon.2024.e34242.
27. A. A. Alzubi, “Lumpy Skin Disease Detection in Cattle by a Robust Approach using Advanced Convolutional Neural Networks,” Indian J. Anim. Res., vol. 58, no. 12, pp. 2146–2153, 2024, doi: 10.18805/IJAR.BF-1793.Submitted.
28. S. M. Saqib et al., “Lumpy skin disease diagnosis in cattle: A deep learning approach optimized with RMSProp and MobileNetV2,” PLoS One, vol. 19, no. 8, pp. 1–16, 2024, doi: 10.1371/journal.pone.0302862.
29. M. Kumar, A. Garg, R. Kumar, A. Singh, and A. Khamparia, “Leveraging Deep Learning for the Detection of Lumpy Skin Disease in Cattle: A New Era in Veterinary Healthcare,” A. Swaroop, V. Kansal, and A. E. Hassanien, Eds., Singapore: Springer Nature Singapore, 2026, pp. 289–300.
30. G. R. Reddy, S. Jaffar, H. Penubaka, and B. L. Jayasree, “Deep Learning-Based Identification of High-Risk Zones for Lumpy Skin Disease in Cattle,” pp. 156–167, 2025, doi: 10.5281/zenodo.15005382.
31. S. Kumar and S. Shastri, “Lumpy Skin Images Dataset,” Mendeley Data. [Online]. Available: https://data.mendeley.com/datasets/w36hpf86j2/1
32. S. Agarwal, “Cow lumpy disease dataset.” [Online]. Available: https://www.kaggle.com/datasets/shivamagarwal29/cow-lumpy-disease-dataset
33. Devang, “Cattle diseases datasets.” [Online]. Available: https://www.kaggle.com/datasets/devang03mgr/cattle-diseases-datasets?select=Cows+datasets

34. A. Jeevan and B. Veena, “CONVOLUTIONAL NEURAL NETWORK APPROACH FOR EARLY DETECTION OF LUMPY SKIN DISEASE,” Int. J. Progress. Res. Eng. Manag. Sci., vol. 05, no. 8, pp. 1774–1778, 2025.
35. T. Velugoti, S. B. Dasari, and S. S. Sultana, “Lumpy Skin Disease Detection Using Deep Learning,” 2024 IEEE Students Conf. Eng. Syst., pp. 1–6, 2024, doi: 10.1109/SCES61914.2024.10652331.